Los Alamos Environmental Restoration Records Processing Facility

ER Record I.D.# 59371

*LOS ALAMOS NATIONAL LABORATORY*
*ENVIRONMENTAL RESTORATION*
*Records Processing Facility*
*ER Records Index Form*

*ER ID NO.* 59371 *Date Received:* 9/25/98 *Processor:* YCA *Page Count:* 17

*Privileged: (Y/N)* N *Record Category:* P *Record Package No:* 0

*FileFolder:* N/A

*Correction: (Y/N)* N *Corrected No.* 0 *Corrected By Number:* 0

*Administrative Record: (Y/N)* Y

*Refilmed: (Y/N)* N *Old ER ID Number:* 0 *New ER ID Number:* 0

*Miscellaneous Comments:*
REFERENCE CITED

14029

*THIS FORM IS SUBJECT TO CHANGE. CONTACT THE RPF FOR LATEST VERSION. (JUNE 1997)*

LA-UR- 97-3924

Approved for public release; distribution is unlimited.

(17)

59371

Title: VADOSE ZONE WATER MOVEMENT AT TA-49, LOS ALAMOS NATIONAL LABORATORY: INTERPRETATIONS BASED ON CHLORIDE AND STABLE ISOTOPE PROFILES

Author(s): Brent D. Newman, EES-15
Robert H. Gilkeson, Weirich & Assoc.
Bruce M. Gallaher, ESH-18

Submitted to: LANL-Internal Report

Received by ER-RPF
SEP 25 1998
MA

Los Alamos
NATIONAL LABORATORY

Los Alamos National Laboratory, an affirmative action/equal opportunity employer, is operated by the University of California for the U.S. Department of Energy under contract W-7405-ENG-36. By acceptance of this article, the publisher recognizes that the U.S. Government retains a nonexclusive, royalty-free license to publish or reproduce the published form of this contribution, or to allow others to do so, for U.S. Government purposes. Los Alamos National Laboratory requests that the publisher identify this article as work performed under the auspices of the U.S. Department of Energy. The Los Alamos National Laboratory strongly supports academic freedom and a researcher's right to publish; as an institution, however, the Laboratory does not endorse the viewpoint of a publication or guarantee its technical correctness.

Form 836 (10/96)

# Vadose Zone Water Movement at TA-49, Los Alamos National Laboratory: Interpretations Based on Chloride and Stable Isotope Profiles

Brent D. Newman[1], Robert H. Gilkeson[2] and Bruce M. Gallaher[3]

September 25, 1997

[1]Environmental Science Group, Los Alamos National Laboratory

[2]Weirich and Associates, Inc., Albuquerque, NM

[3]Water Quality and Hydrology Group, Los Alamos National Laboratory

## ABSTRACT

Natural chloride and stable isotope tracers were used to examine the vadose zone hydrology at boreholes 49-2-700-1 and TDBM-1 at TA-49, Los Alamos National Laboratory. Pore-water chloride concentrations were measured with depth from core samples from both boreholes, and pore water $\delta^{18}O$ and $\delta D$ values were measured for borehole 49-2-700-1. The objectives of the study were to (1) quantify flux rates and pore water ages using the chloride data; (2) examine the chloride and stable isotope profiles for evidence of deep evaporation in the mesa system; and (3) provide data and conceptual information for future modeling activities. Flux rates in the boreholes above the contact between Bandelier Tuff units 1v and 1g range from 0.01 to 0.2 cm/yr. Higher rates were obtained for units below the 1v-1g contact in borehole 49-2-700-1; these ranged from 0.24 to 1 cm/yr. The deeper rates are likely apparent fluxes and may represent past conditions during the early Holocene and late Pleistocene. Chloride-based pore water ages in borehole 49-2-700-1 were about 7000 years at the 1v-1g contact and about 10000 years near the bottom of the hole (692 ft). The chloride-based age for borehole TDBM-1 was about 5000 years at the 109-ft depth, which was the deepest sample analyzed. The chloride bulges in both profiles are consistent with deep- as opposed to surface-evaporation effects. In other words, water is being removed from the mesa tens to hundreds of feet below the surface via vertical or horizontal fractures, or through high-permeability zones that are exposed on the mesa sides. Borehole 49-2-700-1 has occurrences of isotopically heavy

water below 50 ft, which are also indicative of deep evaporation. In addition, some of these heavy water occurrences are coincident with zones of apparent moisture gradient reversals determined previously. A lower flux rate in borehole TDBM-1 was observed for the bottom of unit 4 and the top of unit 3 compared to the rate for the same interval in 49-2-700-1. This difference is likely the result of higher evaporation rates in the vicinity of TDBM-1. The borehole is located near the edge of Frijoles mesa that may result in more evaporative drying of the subsurface. Finally, it appears that the part of the mesa that rises above the elevation of adjacent canyon bottoms is prone to higher rates of evaporative removal of pore waters than units below the elevation of the canyon bottoms.

## INTRODUCTION

Hydrologic processes in deep vadose zones such as at TA-49 are inherently difficult to measure and understand. Yet, because contaminants can potentially move into and through these zones we must be able to estimate flux rates and determine the pathway(s) by which water movement occurs. Among the better techniques for understanding vadose zone behavior are environmental tracer methods. Specifically, natural chloride and stable isotopes have been shown to be particularly useful for estimating vertical flux rates of water and for examining the timing and pathway(s) of water movement in the vadose zone (Allison et al., 1994 and Phillips, 1995). We have

constructed vertical chloride profiles from boreholes 49-2-700-1 and TDBM-1 and measured stable isotopes ($\delta D$ and $\delta^{18}O$) in vadose zone waters from borehole 700-1 in order to understand the natural vadose zone hydrology at TA-49. The objectives of the study were to (1) estimate flux rates and pore water ages using the chloride data; (2) examine the chloride and stable isotope profiles for evidence of deep evaporation in the mesa system; and (3) provide data and conceptual information for future modeling activities. It is assumed that the hydrology in the vicinity of the boreholes has not been influenced by the asphalt pad at TA-49, and thus represents the natural hydrologic behavior of Frijoles Mesa. Borehole 700-1 is close to the asphalt pad, however moisture contents in the borehole are much dryer than those immediately beneath the pad.

Flux rates and pore water ages were determined using the chloride mass balance method (Allison et al., 1994; Stone, 1984). This method provides information not only on the vertical flux rates, but can also be used to examine how flux rates change with depth. Understanding the spatial changes in flux rates is important for assessing how the various Bandelier Tuff units affect flow in the mesa.

Deep evaporation through high permeability zones exposed the sides of the mesa or through fractures, has been suggested by Neeper and Gilkeson (1996) to be an important process at TA-49 based on moisture content measurements and gradient calculations. This process has also been suggested to be important at TA-54, Area G (Rogers and Gallaher, 1995 and

Neeper and Gilkeson, 1996). Understanding whether deep evaporation occurs is important for developing a conceptual model of the TA-49 vadose zone and for understanding why low moisture content zones (and presumably low flux zones) develop within the mesa environment. Stable isotopes can be used to evaluate evaporation, both at the mesa surface and at depth. The isotopic composition of water is affected by evaporation, which preferentially extracts light isotopes into the vapor phase, leaving the remaining liquid enriched in heavy isotopes. If deep evaporation occurs, isotopically heavy pore waters should exist below the shallow zone influenced by surface evaporation.

## MATERIALS AND METHODS

### Chloride Sampling and Laboratory Analyses

Chloride profiles were determined from core samples from boreholes 49-2-700-1 and TDBM-1 at TA-49 (locations are shown in Figure 1). Borehole 49-2-700-1 is a 700-ft hole and is described in Stimac et al. (1997, this report). Borehole TDBM-1 is a 139-ft hole and is described in Purtymun (1995). Samples were collected and analyzed at approximately 5-, 10-, or 20-ft intervals. Chloride concentrations were determined by leaching the core samples with deionized water and analyzing the leachate using ion chromatography. The leaching and analyses were performed at the Los Alamos EES-1 geochemistry laboratory. For each sample, approximately 50 g of tuff was crushed using a mortar and pestle. The tuff was then oven dried for at least 12 hours at 100°C. The dry sample was weighed and added to an

Erlenmeyer flask along with approximately 75-g of DI water. The flask was agitated for 24 hours on a rotary mixer. Once the mixer was turned off and the solid material settled, the supernatant was filtered and analyzed using a Dionex Ion Chromatograph. Analytical precision of the ion chromatograph is better than 5 %.

Pore water chloride concentrations were calculated using the leachate concentrations, gravimetric moisture contents, and bulk densities for each borehole (see Appendices 1a and 1b). Moisture content and bulk density data for borehole 700-1 are from Springer et al. (1997, this report). Moisture content data for borehole TDBM-1 are from Gallaher (1997). Bulk density was not measured for the TDBM-1 cores, so values from 700-1 were used instead. The pore water chloride concentrations were then used in the chloride mass balance approach described below to estimate vertical fluxes and vadose water ages.

## Chloride Mass Balance Approach

The chloride mass balance approach has been successfully used to determine vadose zone fluxes in semiarid and arid locations worldwide. The approach involves measuring chloride concentrations in vadose zone water with depth. These concentrations serve as indicators of downward flux and water age (Stone, 1984; Allison et al., 1994). The downward flux is inversely proportional to the amount of chloride accumulation: high chloride concentrations indicate a low flux that represents many years of meteoric

chloride accumulation coupled with evapotranspirative removal of water. Relatively low chloride contents indicate a high downward flux, or water that is able to move through the vadose zone at a fast enough rate to minimize evapotranspiration effects.

The chloride mass balance method is based on the following assumptions: 1) flow occurs largely as downward piston flow; 2) dispersive mixing of water and chloride is small; 3) atmospheric chloride deposition has been relatively constant and is the sole source of chloride to the system; and 4) chloride uptake by plants is negligible.

If vadose zone chloride concentrations are constant below the root zone, then the average annual flux (or recharge rate) can be estimated using

$$R = P \cdot Cl_p / Cl_{sw}, \qquad (1)$$

where R is the flux (m/yr); P is the average annual precipitation rate (m/yr); $Cl_p$ is the average concentration of chloride in bulk precipitation (g/m$^3$); and $Cl_{sw}$ is the chloride concentration in vadose-zone water below the root zone (g/m$^3$). However, chloride concentrations in deep profiles are sometimes not constant below the root zone (e.g., recharge rates can change over time as a result of climate or land use changes). In this case, plots of cumulative chloride as a function of cumulative water in the profile can be used to determine changes in recharge rates. Approximately linear segments on the cumulative-cumulative plots indicate zones of constant flux. The flux for a segment is given by

$$R = (Cl_p \cdot P)/Cl_{avg}, \quad (2)$$

where $Cl_{avg}$ is the average chloride content of the samples represented by the segment ($g/m^3$). Chloride-based vadose water ages can also be estimated by first calculating the amount of chloride in each sample interval down to the depth of interest using the relationship

$$Cl_i = \theta \cdot C_{cl} \cdot Z \quad (3)$$

where $Cl_i$ is the amount of chloride in the interval ($g/m^2$), $\theta$ is the volumetric moisture content in the interval, $C_{cl}$ is the mass of chloride in the interval per volume of rock ($g/m^3$), and Z is the length of the sample interval (m). By calculating the cumulative sum of the $Cl_i$ values down to the depth of interest, the age can be calculated using

$$A = Cl_{cum}/(Cl_p \cdot P), \quad (4)$$

where A is age in years, and $Cl_{cum}$ is the cumulative sum of the $Cl_i$ values ($g/m^2$) at a given depth. A value of 0.4 m/yr was used for the average annual precipitation (P) based on data in Bowen (1990), and a value of 0.29 $g/m^3$ was used for the average concentration of chloride in bulk precipitation ($Cl_p$) based on data in Anderholm (1994).

Stable Isotope Analyses

Stable isotope analyses of pore waters from TA-49 were conducted using moisture-protected samples archived from the 49-2-700-1 borehole. The moisture-protect system involves sealing core samples in Lexan tubes. This

procedure reduces the chance of pore water evaporation during the period between sampling and analysis, which would alter the isotopic composition of the water. Unfortunately, caps on several of the tubes were not installed properly and evaporative loss of water occurred during storage. As a result, the isotope data set is sparse with no values deeper than 438 ft.

The stable-isotope analyses were carried out at the New Mexico Tech Stable Isotope Laboratory. Soil water was extracted by high-temperature vacuum distillation, following Shurbaji et al. (1995). The $\delta^{18}O$ and $\delta D$ measurements were made on a Finnegan-Mat, Delta-E stable-isotope-ratio mass spectrometer using OZ-Tech gas standards. The hydrogen and oxygen isotopes are reported in delta ($\delta$) notation as per mil (‰) differences relative to the Vienna-Standard Mean Ocean Water (V-SMOW) isotope standard:

$$\delta D \text{ or } \delta^{18}O = \left[\frac{R_{sample} - R_{V\text{-}SMOW}}{R_{V\text{-}SMOW}}\right] \times 1000, \qquad (5)$$

where R is the D/H or $^{18}O/^{16}O$ ratio. The value of $\delta^{18}O$ was measured from extractions made using the carbon dioxide equilibration technique of Socki et al. (1992). For the $\delta D$ analyses, hydrogen was extracted using the hot uranium method of Bigeleisen et al. (1952). The analytical precision for the $\delta^{18}O$ and $\delta D$ analyses by mass spectroscopy is better than ±0.2 ‰ and ±6 ‰, respectively.

## RESULTS

Chloride profiles for the two boreholes are shown in Figure 2. The 49-2-700-1 profile shows bulges of high concentration between the 0-25 ft and 160-380 ft depths. The TDBM-1 profile shows generally high chloride concentrations throughout the 100-ft interval. The major changes in chloride concentrations in borehole 49-2-700-1 correspond to changes in gravimetric moisture content where the chloride bulges occur in the zone of low moisture content (Figure 3).

Because the chloride concentrations were not constant with depth, the cumulative chloride-cumulative water approach was used to calculate fluxes (values used in the flux and age calculations are given in Appendix 1). Cumulative-cumulative plots for the boreholes are shown in Figure 4. The figures show multiple linear segments. For borehole 49-2-700-1 the break in slope between the third and fourth segments corresponds closely to the 1v-1g contact (this contact is equivalent to the outcrop feature known as the vapor phase notch). The break between the fourth and fifth segments corresponds to the Tsankawi Pumice Bed. Flux rates were calculated for the five segments in 49-2-700-1 and for the two segments in TDBM-1 (Table 1).

Chloride accumulation ages for each borehole are also shown in Table 1. Ages for borehole 49-2-700-1 suggest that it takes about 7000 years to reach the 1v-1g contact and about 10000 years to reach the bottom of the hole. Ages for TDBM-1 suggest that it takes approximately 5000 years to reach the 109-ft depth (unit 3). The differences in chloride-based flux rates and ages indicate

water movement though the 0-100 ft depth range in TDBM-1 is slower than in 49-2-700-1.

The stable isotope data for borehole 49-2-700-1 are shown in Table 2 . Most of the waters have been subject to evaporative processes because they plot to the right of the local meteoric water line (Figure 5). The water samples that plot closest to the local meteoric water line are from the area of the 1v-1g contact. The isotopic composition of standing water from borehole CH-2 (a 150-ft borehole at the TA-49 asphalt pad) is also plotted. The CH-2 water is isotopically different from the borehole 49-2-700-1 waters supporting the assumption that the asphalt pad has not influenced the 49-2-700-1 hydrology.

## DISCUSSION

### Significance of the Chloride Bulges

The chloride bulges (Figure 1) are important features of the vertical profiles because the origin of these chloride accumulations will affect the development of conceptual and quantitative models of the mesa hydrologic system. One explanation is that the bulges represent a past period of low percolation rates and high evapotranspiration, which was, followed by a period of higher percolation rates and lower evapotranspiration that displaced much of the chloride to depths far below the root zone. However, the vadose water ages for the bulges are not concordant between boreholes 49-2-700-1 and TDBM-1. If changing paleoclimate was the main cause of the chloride bulges,

roughly similar chloride concentrations and ages would be expected. A further problem is that the early- to mid-Holocene was apparently a wetter or higher recharge period than the present (Markgraf et al., 1983; Phillips et al., 1986). This is in direct contrast to the interpretation that the bulges indicate drier past conditions. The most likely explanation is that the bulges represent zones of evaporation and vapor phase transport of water, which would cause chloride to accumulate. The possible pathways of vapor movement are discussed in the Stable Isotope section below. The deep evaporation interpretation is supported by other studies that have suggested the possible presence of deep zones of vapor dominated transport (e.g., Neeper and Gilkeson, 1996; Rogers and Gallaher, 1995; Rogers et al., 1996; and Vold et al. 1997). The differences in chloride accumulation between the boreholes suggests that if evaporation occurs, there may be substantial lateral heterogeneity where the evaporative flux is not uniform throughout the mesa. Borehole TDBM-1 contains more chloride in the top 100 ft than does 49-2-700-1. TDBM-1 is much closer to edge of the mesa and the mesa side has better exposures of the shallower units than occurs near 49-2-700-1. These factors would promote more evaporation at TDBM-1 than at 49-2-700-1.

The changes in chloride and flux rates in borehole 49-2-700-1 appear to be correlated to certain stratigraphic units and features. The low flux zone at the bottom of unit 3 through the top of unit 1v (Figure 4, Table 1) is consistent with a low flux zone in units 2 and 1v at TA-54, MDA G (Newman, 1997) even

though these units occur some 60 ft deeper at TA-49 than Area G. This consistency of high chloride inventories in certain stratigraphic units in two different mesas suggests that unit 2 and the top of unit 1v are well connected to the atmosphere. The surge beds in unit 2 have been suggested as a potential evaporative zone (Rogers and Gallaher, 1995; Rogers et al., 1996), and the lithologic contacts between subunits of 1v may also provide an atmospheric connection.

The 1v-1g contact is another stratigraphic feature that appears to control or at least correlate with changes in chloride concentrations and flux rates both at TA-49 and Area G. At borehole 49-2-700-1, chloride concentrations at and below the contact are dilute and the decrease in concentration corresponds to a substantial increase in moisture content (Figure 3). A similar change in flux rates occurs below the Tsankawi Pumice Bed where moisture contents increase further. The wetter conditions in the units below the 1v-1g contact are likely due to terrain effects because these units are below the canyon bottom and are probably not subject to the same evaporative processes as the above canyon parts of the mesa. It thus appears that the stratigraphic contacts and their position relative to the canyon bottoms play an important role in the mesa moisture and flux distribution. The coincidence of changes in flux with stratigraphic contacts, in addition to any changes in evaporative processes, is probably the result of sharp transitions in hydrologic properties. This interpretation is supported by the work of Gilkeson et al. (1996) who noted a large change in tuff surface area at the 1v-1g contact in borehole 49-2-700-1.

Because there is likely an evaporative sink in Frijoles Mesa, the high flux rates for the units below the 1v-1g contact do not make sense from a mass balance standpoint, assuming there is no additional source of water at depth. The rates, therefore, are apparent rates, and the early Holocene to late Pleistocene chloride-based ages of the deep waters suggest that they are relict. Thus, instead of reflecting current rates, the rates below the 1v-1g contact may represent paleoflux rates during the early Holocene and late Pleistocene.

Uncertainty

With the various assumptions used in the chloride mass balance method there are some related uncertainties. The first uncertainty relates to the 1-D vertical flow assumption. If deep evaporative processes occur, then potentially large but unquantifiable errors in the flux estimates result. From a qualitative point of view, however, a large chloride concentration associated with an evaporative zone is consistent with a low flux. Fracture flow is not considered in the chloride mass balance approach and because of its possible importance, especially in the shallower tuff units, this adds additional uncertainty to the flux and age estimates. The 1-D flow assumption may also be violated as a result of spatially varying hydrologic properties that can cause lateral flow. A modeling study by McCord et al. (1997) suggests that failure to account for geologic heterogeneity can result in an overestimation of flux rates by a factor of 3 or 4. Another factor that contributes to uncertainty is the concentration of chloride entering the mesa. Unfortunately, there are no long-term data

available for the Los Alamos area, but short-term data can be used to bound the problem. A value of 0.29 g/m$^3$ was used in the flux and age calculations based on a chloride mass balance study by Anderholm (1994) for the Santa Fe area. This value may be higher than the actual Pajarito Plateau average, and is thus conservative in that if it is a high value, flux rates will be overestimated and ages underestimated. Evaluation of chloride concentrations in precipitation from the National Atmospheric Deposition Program station at Bandelier National Monument (NADP, 1994) and various sampling stations on the Pajarito Plateau monitored by Adams et al. (1995) suggest that average annual chloride concentrations in rainfall might be as low as 0.1 g/m$^3$. If this value is more representative of the Pajarito Plateau, then the fluxes in Table 1 would be about one third less than those shown and the ages would be about three times greater. The different chloride input values do not make order of magnitude changes in the flux rates, and thus do not result in much additional uncertainty, especially when compared to uncertainties from other factors such as deep evaporation. The effect of different chloride concentrations however, can be an important consideration for correlating ages and changes in flux with past periods of climate change because some paleoclimate changes have occurred over relatively short time periods. In summary, there are a number of factors that contribute to uncertainty in the flux and age estimates. However, the bias is to overestimate flux and underestimate ages. In the case of environmental problems, this bias is not a great problem because it results in conservative estimates of water movement.

Stable Isotopes

Stable isotope data from borehole 49-2-700-1 (Figure 4) provide additional evidence for deep evaporation. Shallow stable isotope profiles measured at TA-69 and TA-51 by Newman et al. (1997) indicate that surface evaporation effects disappear at depths less than 6 ft whereupon values reach relatively light $\delta^{18}O$ and $\delta D$ values of -9 to -10 ‰ and -80 to -95 ‰, respectively. Vadose zone stable isotope theory predicts that a quasi-steady state value should be reached below the zone influenced by solar surface evaporation (Allison et al., 1983; Barnes and Allison, 1983). In other words, the approximately -9 ‰ $\delta^{18}O$ value, for example, should be maintained throughout the profile for all depths below about 6 ft. However, contrary to theory, the 49-2-700-1 data show heavy values at depths below the zone influenced by surface evaporation (Table 2).

A paleoclimate interpretation for the existence of isotopically heavy values deep in the profile does not seem plausible, as explained in the chloride bulge discussion. Instead, the isotope data are consistent with evaporative removal of water from within the mesa. Neeper and Gilkeson (1996) found apparent reversed moisture gradients at approximately the 225 and 310 ft depths. The isotope data show heavy values of -5‰, -66‰ and -3‰, -57‰, $\delta^{18}O$ and $\delta D$ respectively, at the same depths as the "reversed gradients" of Neeper and Gilkeson. The correlation between the reversed gradients and heavy isotope values strongly suggests that deep evaporation occurs at these

zones. It should be noted that other isotopically heavy values were observed for the 85, 361, and 439-ft depths (Table 2). "Reversed gradients" may also occur at these depths. At present, it is not clear how the evaporative process works or what the pathways for airflow and water removal might be. One hypothesis is that dry air travels down vertical fractures in the tuff, evaporates the water and moves back out of the fractures in response to thermal or barometric changes. Alternatively, the sides of the mesa could play a role in allowing dry air into the system and moving water vapor laterally out. The Bandelier tuff is exposed on the mesa sides and is subject to a wide range of temperatures and barometric pressures. The lateral pathway appears to be the most likely because units 2 and 1v appear to be evaporative zones at both TA-49 and Area G, but occur at different depths in the two mesas. The tracers, low moisture contents, and gradient data strongly indicate that deep evaporation occurs in the mesas at TA-49 and Area G. However, additional work will be required to understand the mechanisms and pathways by which evaporation occurs.

The existence of light isotope values at the 1v-1g contact in borehole 49-2-700-1 leads to two explanations. The first explanation is that water infiltrated during a higher precipitation period during the Pleistocene or early to mid Holocene, and was not subject to extensive evaporation. Studies by Markgraf (1983) and Phillips et al. (1986) indicate that such periods occurred in the past 20,000 years, so this explanation appears to be reasonable for the light water at the bottom of the profile. Another possibility is that water may

have been introduced by lateral flow along pathways that were not subject to evaporation of the same intensity that occurred in the middle of the mesa. It is possible that alluvial water from Water Canyon flows underneath TA-49. Unfortunately, we do not have enough information about the link between mesa and canyon hydrology to adequately evaluate if lateral flow really occurs. The stable isotope data however, can provide clues regarding the validity of the lateral flow hypothesis. The meteoric water plot (Figure 5) shows an evaporation trend line extending from the local meteoric water line to the right. $\delta^{18}O$ and $\delta D$ values of precipitation from the Pajarito Plateau plot along the local meteoric water line, and if evaporation occurs the isotopic values will become progressively heavier following a trend such as that shown for borehole 49-2-700-1. The evaporative trend line suggests that the waters in the 49-2-700-1 profile have the same source, including the light water at the 1v-1g contact. Thus, if lateral flow occurs, it would have to have the same original isotopic composition as the water that was evaporated from the middle of the mesa. In other words, the source of the lateral flow would need to plot on the same evaporation trend line as the 49-2-700-1 waters. Measurements of the isotopic composition of potential lateral flow sources, such as alluvial groundwater from Water Canyon, would greatly aid in resolving this question.

## SUMMARY AND CONCLUSIONS

Chloride based flux estimates for the zone above the 1v-1g contact for boreholes 49-2-700-1 and TDBM-1 range from 0.01to 0.2 cm/yr. These low

flux rates are likely the result of evaporative removal of water in the mesa. Heavy stable isotope values from borehole 49-2-700-1 support this interpretation. Flux estimates for the zone below the 1v-1g contact in borehole 49-2-700-1 range from 0.24 to 1 cm/yr. These deeper rates are likely apparent flux rates and may represent past conditions during the late Pleistocene and early Holocene. Chloride profiles for the two boreholes showed similar behavior in the top 30 ft. Below this depth, TDBM-1 shows a greater accumulation of chloride in unit 3 than borehole 49-2-700-1 and indicates that water moves more slowly in the vicinity of TDBM-1. The difference in chloride concentrations and flux rates is probably caused by higher evaporation rates at TDBM-1 as a result of its close location to the side of Frijoles mesa.

## ACKNOWLEDGMENTS

Funding for this research was provided through the LANL Area G Performance Assessment, and the interest and support of Diana Hollis is particularly appreciated. The LANL Environmental Surveillance Program provided funding for the TDBM-1 chloride work. The authors would like to thank Dale Counce for performing the leachings and chloride analyses, and Andrew Campbell and Christa Vindum for their work on the stable isotope analyses. Bennie Martinez is also thanked for providing the isotope data for well CH-2. A review by Jack Nyhan was greatly appreciated.

## REFERENCES


Adams, A. I., F. Goff and D. Counce. 1995. Chemical and Isotopic Variations of Precipitation in the Los Alamos Region, New Mexico. Los Alamos National Laboratory Report, LA-12895-MS. 35 pp.

Allison, G. B., Barnes, C. J. and Hughes, M. W. 1983. The Distribution of Deuterium and $^{18}O$ in Dry Soils 2: Experimental. J. Hydrol. 64: 377-397.

Allison, G. B., G. W. Gee, and S. W. Tyler. 1994. Vadose-Zone Techniques for Estimating Groundwater Recharge in Arid and Semiarid Regions. Soil Sci. Soc. of Am. J. V. 58. pp. 6-14

Anderholm, S. K. 1994. Ground-water Recharge Near Santa Fe, North-Central New Mexico. USGS Water-Res. Invest. Rep. 94-4078. 68 pp.

Barnes, C. J., and Allison, G. B., 1983. The Distribution of Deuterium and $^{18}O$ in Dry Soils. 1. Theory. J. Hydrol., 60: 141-156.

Bigeleisen, J., M. L. Perlman, H. C. Prosser. 1952. Conversion of Hydrogenic Materials to Hydrogen for Isotopic Analysis. Anal. Chem., V. 24. pp. 1356-1357.

Bowen, B. M. 1990. Los Alamos Climatology. Los Alamos National Laboratory Report LA-11735-MS. 254 pp.

Gallaher, B. M. 1997. Unpublished Los Alamos National Laboratory Data.

Gilkeson, R., D. Neeper, M. Ankeny, W. Lowry, D. Krier, and D. Broxton. 1996. Passive Hydraulic Isolation of Waste in Bandelier Tuff. Poster, 8th Annual DOE Technology Information Exchange (TIE) Conference, Santa Fe.

Markgraf, V., J. Platt Bradbury, R. M. Forester, W. McCoy, G. Singh, and R. Sternberg. 1983. Paleoenvironmental Reassessment of the 1.6-Million-Year-Old Record from San Agustin Basin, New Mexico. In C. E. Chapin (ed.) New Mexico Geological Society Guidebook, 34th Field Conference, Socorro Region II. New Mexico Geological Society, Socorro, NM. pp. 291-297.

McCord, J. T., C. A. Gotway, and S. H. Conrad. 1997. Impact of Geologic Heterogeneity on Recharge Estimation Using Environmental Tracers: Numerical Modeling Investigation. Water Res. Research, V. 33, No. 6. Pp. 1229-1240.

National Atmospheric Deposition Program (NADP). 1994. National Trends Network NADP/NTN (NRSP-3) Site Report, Precipitation and Chemistry Data. Natural Resource Ecology Laboratory, Colorado State, Ft. Collins, CO.

Neeper, D. A. and R. H. Gilkeson. 1996. The Influence of Topography, Stratigraphy, and Barometric Venting on the Hydrology of Unsaturated Bandelier Tuff. in Goff, F., Kues, B. S., Rogers, M. A., McFadden, L. D., and Gardner, J. N., eds., The Jemez Mountains region: New Mexico Geological Society Forty-Seventh Annual Field Conference Guidebook. pp. 427-432.

Newman, B. D., 1997. Vadose Zone Water Movement at Area G, Los Alamos National Laboratory, TA-54: Interpretations Based on Chloride and

Stable Isotope Profiles. in D. Hollis et al., Performance Assessment and Composite Analysis for Los Alamos National Laboratory Material Disposal Area G.

Newman, B. D., A. R. Campbell, and B. P. Wilcox. 1997. Tracer-based Studies of Soil Water Movement in Semi-Arid Forests of New Mexico. Journal of Hydrology, in press.

Phillips, F. M. 1995. The Use of Isotopes and Environmental Tracers in Subsurface Hydrology. Rev. of Geophys., Supplement, U.S. National Rep. To the Intern. Union of Geodesy and Geophy. 1991-1994. pp. 1029-1033.

Phillips, F. M., L. A. Peters, M. K. Tansey, and S. N. Davis. 1986. Paleoclimatic Inferences from an Isotopic Investigation of Groundwater in the Central San Juan Basin, New Mexico. Quat. Res. V. 26. pp. 179-193.

Purtymun, W. D. 1995. Geologic and Hydrologic Records of Observation Wells, Supply Wells, Springs, and Surface Water Stations in the Los Alamos Area. Los Alamos National Laboratory Report, LA-12883-MS.

Rogers, D. B, and B. M. Gallaher. 1995. The Unsaturated Hydraulic Characteristics of the Bandelier Tuff. Los Alamos National Laboratory Report, LA-12968-MS.

Rogers, D. B., B. M. Gallaher, and E. L. Vold. 1996. Vadose Zone Infiltration Beneath the Pajarito Plateau at Los Alamos National Laboratory. New Mexico Geological Society 1996 Guidebook, Geology of the Los Alamos-Jemez Mountains Region. In Press.

Shurbaji, A.-R.M., Phillips, F. M., Campbell, A. R. and Knowlton, R. G. 1995. Application of a Numerical Model for Simulating Water Flow, Isotope Transport, and Heat Transfer in the Unsaturated Zone. J. Hydrol. 171: 143-163.

Springer, E. P, R. H. Gilkeson, and L. Hamilton. 1997. (This volume).

Socki, R. A., Karlsson, H. R. and Gibson, E. K. 1992. Extraction Technique for the Determination of Oxygen-18 in Water Using Preevacuated Glass Vials. Anal. Chem., 64: 829-831.

Stimac, J. A., D. E. Broxton, E. C. Kluk, and S. J. Chipera. 1997. Preliminary Stratigraphy of Tuffs From Borehole 49-2-700-1 at Technical Area 49, Los Alamos National Laboratory, New Mexico. (This volume).

Stone, W. J. 1984. Recharge in the Salt Lake Coal Field Based on Chloride in the Unsaturated Zone. New Mexico Bureau of Mines and Mineral Resources, Open-File Report 214. 64 pp.

Vold, E., B. Newman, K. Birdsell, B. Gallaher, D. Krier, P. Longmire, D. Rogers, and E. Springer. 1997. Representative Recharge Rates in a Complex Unsaturated Hydrogeology. in Waste Management '97.

Vuataz, F.-D. and Goff, F. 1986. Isotope Geochemistry of Thermal and Nonthermal Waters in the Valles Caldera, Jemez Mountains, Northern New Mexico. J. Geophys. Res., 91(B2): 1835-1853.

Table 1. Flux estimates and pore water ages for boreholes 49-2-700-1 and TDBM-1.

| Borehole 49-2-700-1 | | | |
|---|---|---|---|
| Depth interval (ft) | Unit | Flux (cm/yr) | Age at bottom of depth interval (yr) |
| 0-23 | Qbt4 | 0.03 | 880 |
| 29-153 | Qbt3, Qbt4 | 0.2 | 1440 |
| 159-344 | Qbt1v, Qbt3 | 0.05 | 6544 |
| 364-539 | Qbt1g, Qbt1v | 0.24 | 9705 |
| 561-692 | Qbo, Qct, Qbt t, Qbt1g | 1 | 10271 |

| Borehole TDBM-1 | | | |
|---|---|---|---|
| Depth interval (ft) | Unit | Flux (cm/yr) | Age at bottom of depth interval (yr) |
| 0-54 | Qbt4, Qbt3 | 0.04 | 1549 |
| 74-109 | Qbt3 | 0.01 | 5227 |

Table 2. Stable isotope compositions of borehole 49-2-700-1 waters.

| Depth (ft) | $\delta^{18}O$ (permil) | $\delta D$ (permil) |
|---|---|---|
| 47.2 | -8.2 | -87 |
| 72 | -8.4 | -86 |
| 85.2 | -5.8 | -81 |
| 95.2 | -8.5 | -75 |
| 120 | -7.8 | -78 |
| 143.6 | -9.2 | -77 |
| 225.0 | -5.1 | -66 |
| 251.6 | -8.0 | -74 |
| 268.8 | -7.7 | -69 |
| 286.8 | -8.5 | -72 |
| 306.8 | -8.5 | -73 |
| 325.8 | -2.7 | -57 |
| 381.4 | -8.4 | -74 |
| 379.8 | -10.1 | -79 |
| 420.2 | -10.7 | -84 |
| 438.8 | -4.5 | -66 |

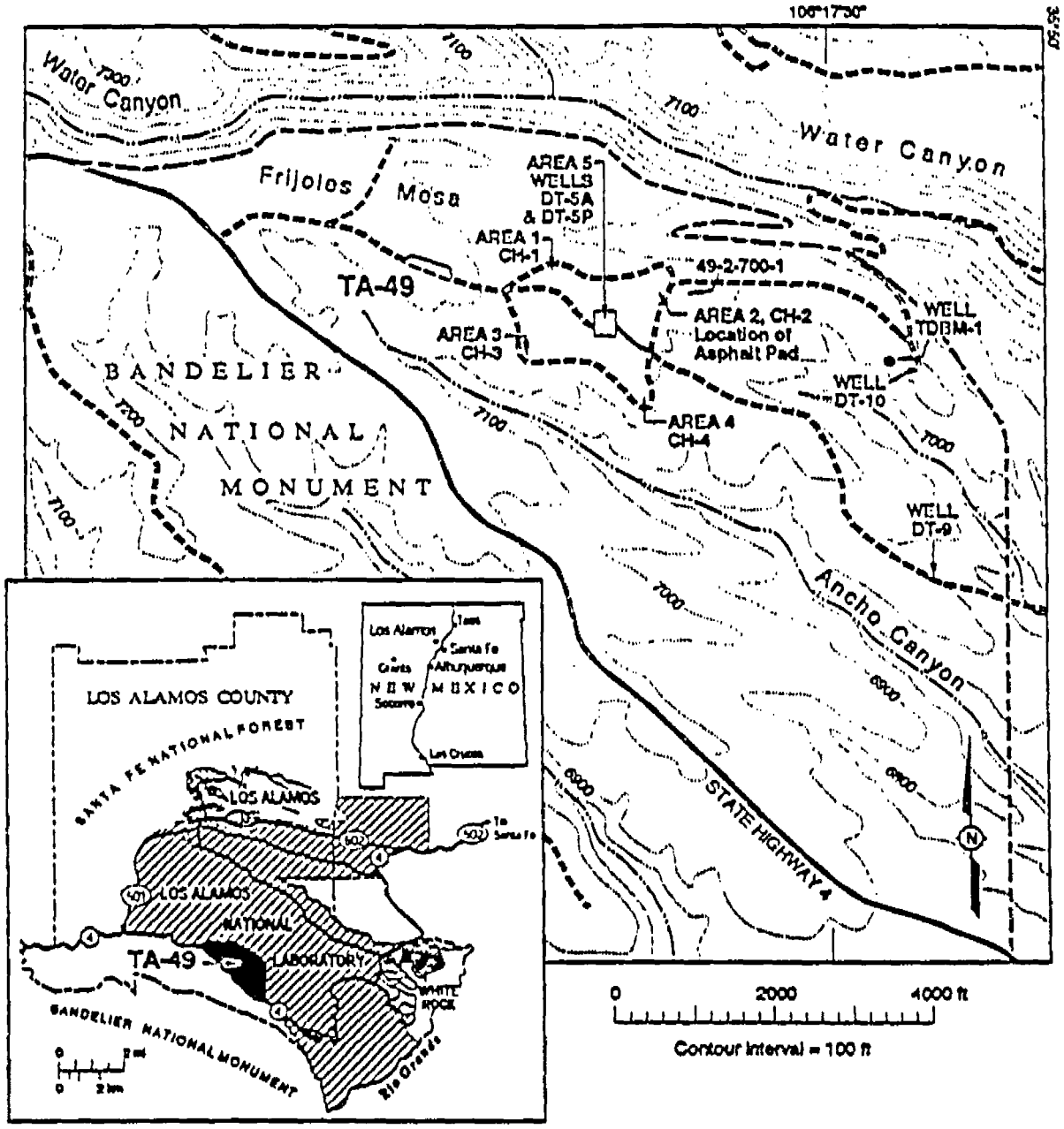


Figure 1. Map of the TA-49 area showing the locations of boreholes 49-2-700-1 and TDBM-1.

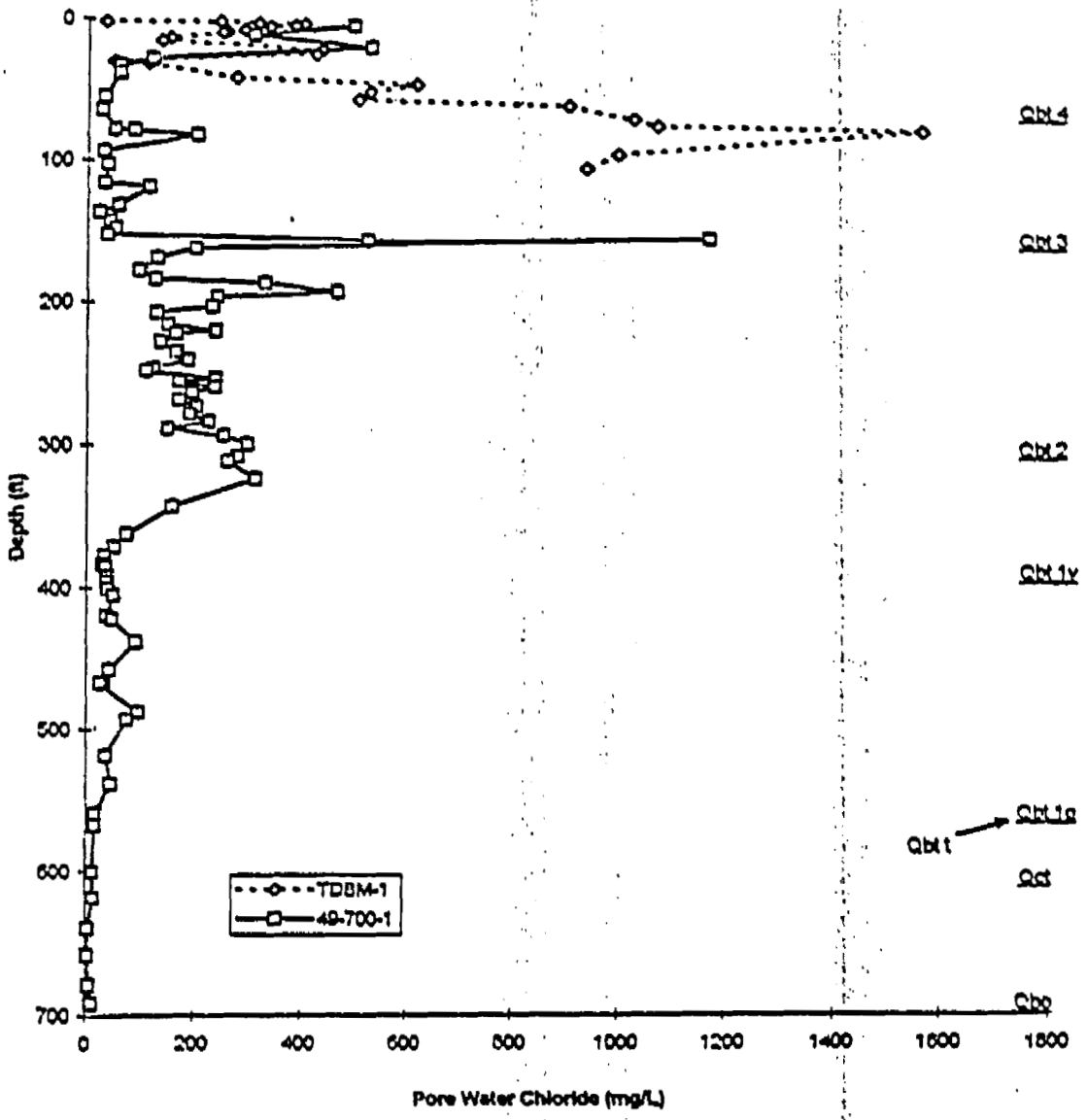


**Figure 2. Pore water chloride in boreholes 49-2-700-1 and TDBM-1. Horizontal lines on the right side of the figure indicate the lower stratigraphic boundary of the given unit.**

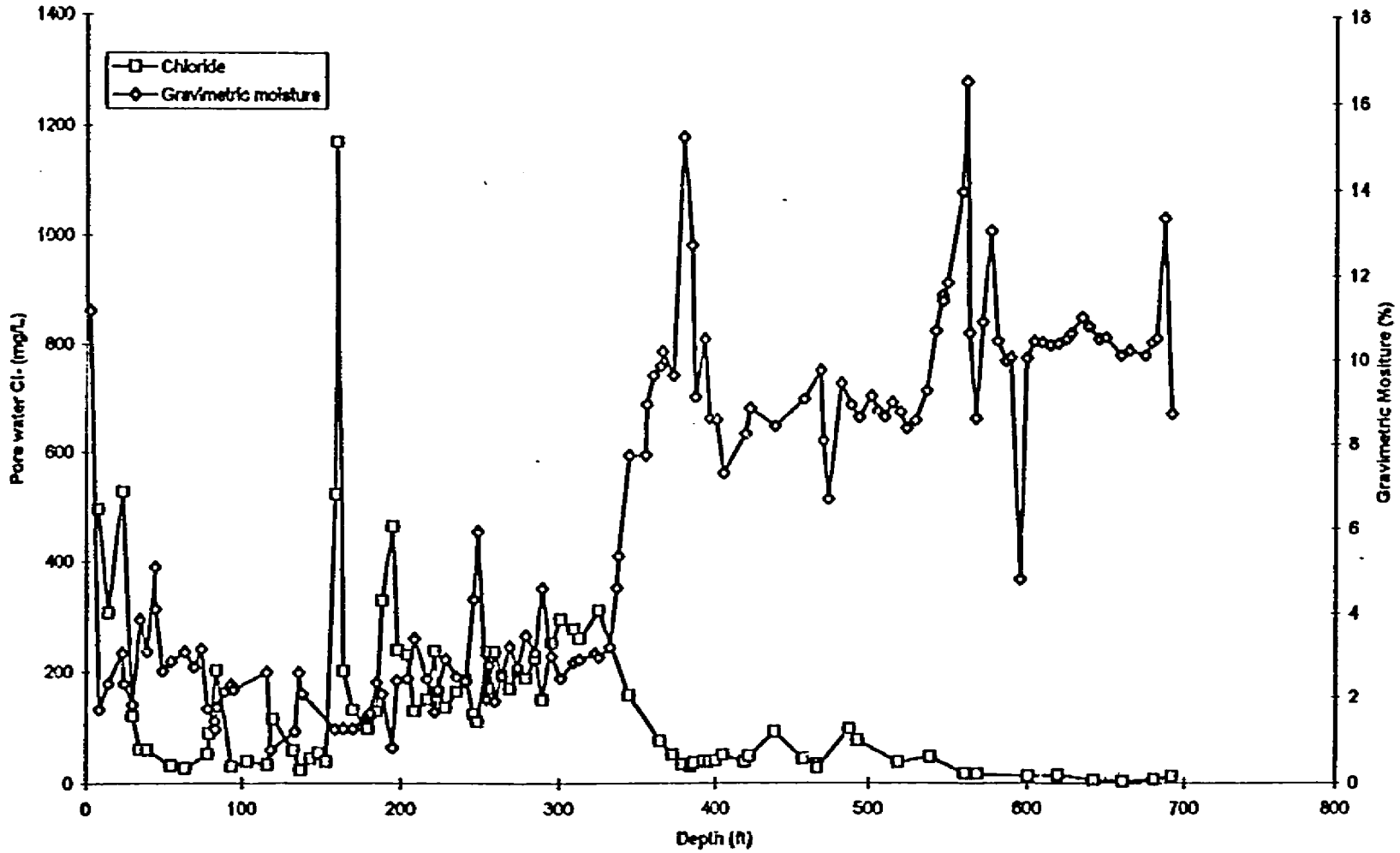


Figure 3. Pore water chloride and gravimetric moisture in borehole 49-2-700-1.

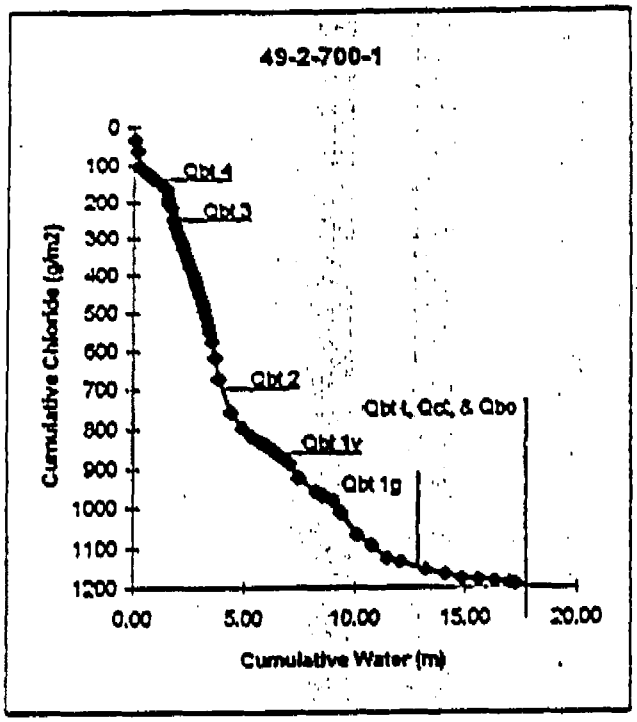


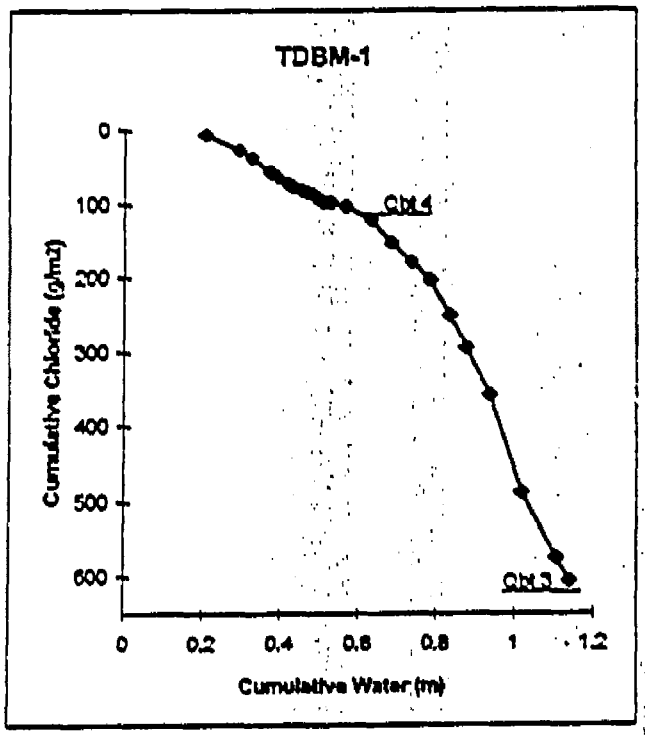


Figure 4. Cumulative water versus cumulative chloride for holes 49-2-700-1 and TDBM-1.

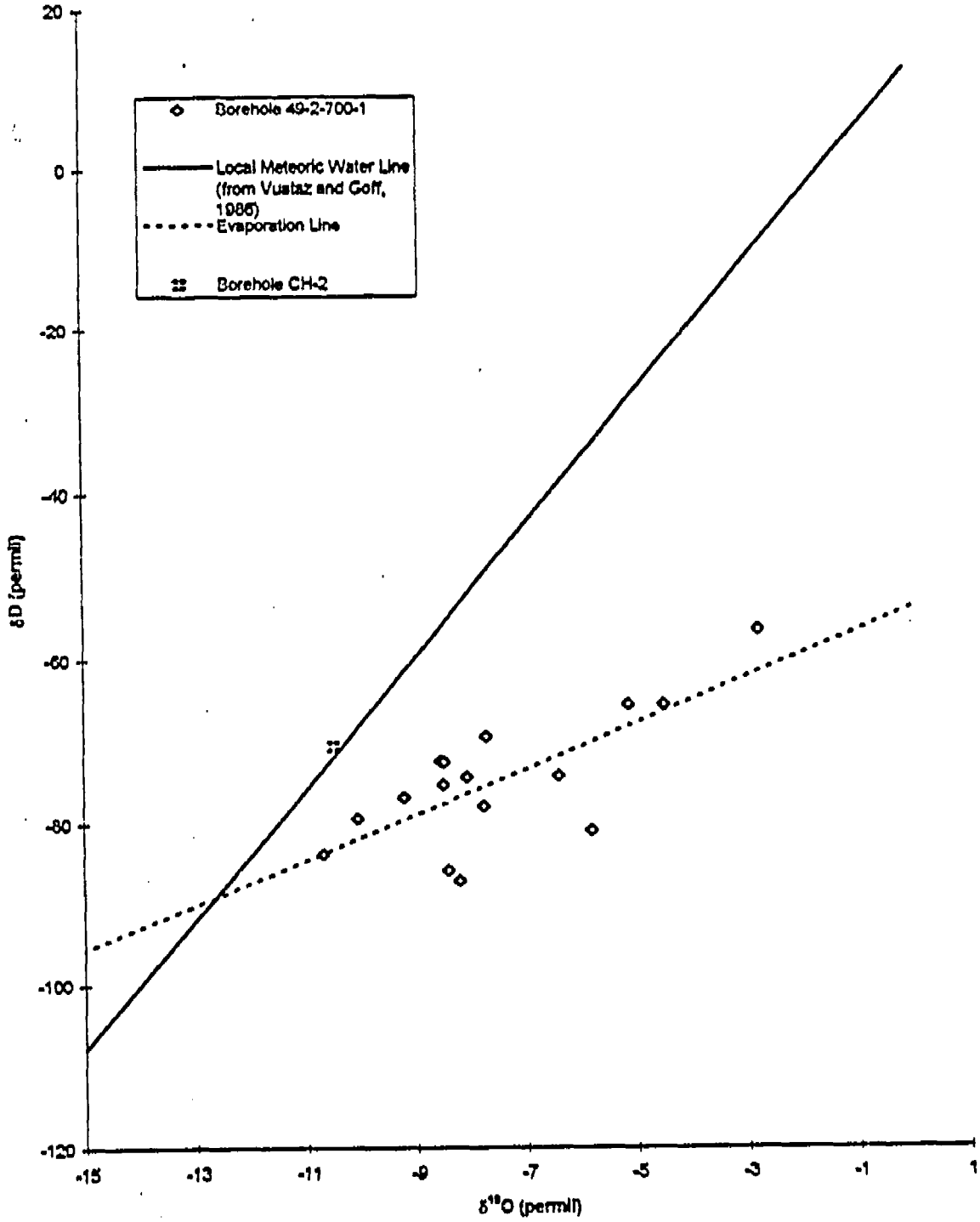


Figure 5. Meteoric water diagram for borehole 49-2-700-1.

Appendix 1a. Borehole 49-2-700-1 chloride mass balance data.

| Depth (ft) | Depth (m) | θg (%) | ρb (g/cm3) | θv (%) | Tuff Dry wt. (g) | Cl- µg/g | Pore H2O (L) | Cl- (mg) | Cl- (mg/L) | Interval (m) | Interval Clswi (g/m2) | Cum. Clswi (g/m2) | Interval θd (m) | Cum θd (m) | Age (yrs) |
|---|---|---|---|---|---|---|---|---|---|---|---|---|---|---|---|
| 7.5 | 2.3 | 1.7 | 1.3 | 2.2 | 79.8 | 8.4 | 0.001 | 0.67 | 497 | 3.0 | 32.9 | 33 | 0.07 | 0.07 | 284 |
| 14.1 | 4.3 | 2.3 | 1.3 | 3.0 | 64.5 | 7.1 | 0.001 | 0.46 | 308 | 3.0 | 27.6 | 61 | 0.09 | 0.2 | 522 |
| 23.5 | 7.2 | 3.02 | 1.3 | 3.9 | 96.6 | 16.0 | 0.003 | 1.54 | 529 | 2.0 | 41.5 | 102 | 0.08 | 0.2 | 880 |
| 29.8 | 9.1 | 1.81 | 1.3 | 2.4 | 95.7 | 2.2 | 0.002 | 0.21 | 119 | 1.5 | 4.2 | 106 | 0.04 | 0.3 | 916 |
| 34.6 | 10.5 | 3.8 | 1.3 | 4.9 | 97.7 | 2.3 | 0.004 | 0.23 | 61 | 1.5 | 4.5 | 111 | 0.07 | 0.3 | 955 |
| 39.2 | 11.9 | 3.05 | 1.3 | 4.0 | 89.4 | 1.8 | 0.003 | 0.16 | 60 | 4.0 | 9.5 | 120 | 0.16 | 0.5 | 1037 |
| 55 | 16.8 | 2.82 | 1.3 | 3.7 | 104.4 | 0.9 | 0.003 | 0.09 | 31 | 3.0 | 3.4 | 124 | 0.11 | 0.6 | 1067 |
| 63.9 | 19.5 | 3.04 | 1.3 | 4.0 | 88.8 | 0.8 | 0.003 | 0.07 | 27 | 3.0 | 3.2 | 127 | 0.12 | 0.7 | 1094 |
| 78.2 | 23.8 | 1.71 | 2 | 3.4 | 106.2 | 0.9 | 0.002 | 0.09 | 52 | 3.0 | 5.3 | 132 | 0.10 | 0.8 | 1140 |
| 79.1 | 24.1 | 1.7 | 1.36 | 2.3 | 46.5 | 1.49 | 0.001 | 0.07 | 88 | 1.0 | 2.0 | 134 | 0.02 | 0.9 | 1158 |
| 83.55 | 25.5 | 1.3 | 1.36 | 1.8 | 48.5 | 2.63 | 0.001 | 0.13 | 202 | 2.0 | 7.2 | 141 | 0.04 | 0.9 | 1219 |
| 93.35 | 28.5 | 2.3 | 1.65 | 3.7 | 48.7 | 0.68 | 0.001 | 0.03 | 30 | 3.0 | 3.4 | 145 | 0.11 | 1.0 | 1248 |
| 103.15 | 31.4 | 2.3 | 1.65 | 3.8 | 51.2 | 0.88 | 0.001 | 0.04 | 38 | 3.0 | 4.3 | 149 | 0.11 | 1.1 | 1286 |
| 116.25 | 35.4 | 2.6 | 1.65 | 4.2 | 54.3 | 0.84 | 0.001 | 0.05 | 33 | 2.5 | 3.5 | 153 | 0.11 | 1.2 | 1316 |
| 119.55 | 36.4 | 0.8 | 1.65 | 1.3 | 47.7 | 0.91 | 0.000 | 0.04 | 114 | 3.0 | 4.5 | 157 | 0.04 | 1.3 | 1355 |
| 132.5 | 40.4 | 1.2 | 1.65 | 1.9 | 53.8 | 0.68 | 0.001 | 0.04 | 57 | 2.0 | 2.2 | 159 | 0.04 | 1.3 | 1374 |
| 136.85 | 41.7 | 2.6 | 1.65 | 4.2 | 60.1 | 0.58 | 0.002 | 0.03 | 23 | 1.0 | 1.0 | 160 | 0.04 | 1.3 | 1382 |
| 143.3 | 43.7 | 2.0 | 1.65 | 3.3 | 51.3 | 0.86 | 0.001 | 0.04 | 43 | 2.0 | 2.8 | 163 | 0.07 | 1.4 | 1406 |
| 148.3 | 45.2 | 1.8 | 1.65 | 2.9 | 49.6 | 0.93 | 0.001 | 0.05 | 53 | 1.5 | 2.3 | 165 | 0.04 | 1.5 | 1426 |
| 153.1 | 46.7 | 1.8 | 1.65 | 2.9 | 58.1 | 0.67 | 0.001 | 0.04 | 38 | 1.5 | 1.7 | 167 | 0.04 | 1.5 | 1441 |
| 159 | 48.5 | 1.23 | 1.65 | 2.0 | 79.8 | 6.45 | 0.001 | 0.51 | 524 | 2.0 | 21.3 | 188 | 0.04 | 1.5 | 1624 |
| 159.2 | 48.5 | 1.23 | 1.65 | 2.0 | 50.2 | 14.4 | 0.001 | 0.72 | 1170 | 0.5 | 11.9 | 200 | 0.01 | 1.5 | 1726 |
| 164 | 50.0 | 1.24 | 1.65 | 2.0 | 112.8 | 2.49 | 0.001 | 0.28 | 201 | 1.0 | 4.1 | 204 | 0.02 | 1.6 | 1762 |
| 170.2 | 51.9 | 1.24 | 1.65 | 2.0 | 113.9 | 1.61 | 0.001 | 0.18 | 130 | 2.0 | 5.3 | 210 | 0.04 | 1.6 | 1807 |
| 179.2 | 54.6 | 1.53 | 1.65 | 2.5 | 104.5 | 1.47 | 0.002 | 0.15 | 96 | 2.0 | 4.9 | 215 | 0.05 | 1.7 | 1849 |
| 185 | 56.4 | 2.32 | 1.86 | 4.3 | 52.6 | 2.94 | 0.001 | 0.15 | 127 | 1.0 | 5.5 | 220 | 0.04 | 1.7 | 1897 |
| 188.7 | 57.5 | 2.05 | 1.86 | 3.8 | 85.2 | 6.77 | 0.002 | 0.58 | 330 | 2.0 | 25.2 | 245 | 0.08 | 1.8 | 2114 |
| 195 | 59.4 | 0.82 | 1.86 | 1.5 | 97.7 | 3.82 | 0.001 | 0.37 | 468 | 1.5 | 10.7 | 256 | 0.02 | 1.8 | 2206 |
| 197.9 | 60.3 | 2.38 | 1.86 | 4.4 | 72.6 | 5.73 | 0.002 | 0.42 | 241 | 1.5 | 16.0 | 272 | 0.07 | 1.9 | 2343 |
| 204.2 | 62.2 | 2.42 | 2.02 | 4.9 | 94.7 | 5.61 | 0.002 | 0.53 | 232 | 1.5 | 17.0 | 289 | 0.07 | 1.9 | 2490 |
| 208.3 | 63.5 | 3.37 | 2.02 | 6.8 | 68.0 | 4.35 | 0.002 | 0.30 | 129 | 1.5 | 13.2 | 302 | 0.10 | 2.0 | 2604 |
| 216 | 65.8 | 2.41 | 2.02 | 4.9 | 93.9 | 3.61 | 0.002 | 0.34 | 150 | 2.0 | 14.6 | 317 | 0.10 | 2.1 | 2729 |

Appendix 1a. Borehole 49-2-700-1 chloride mass balance data.

| Depth (ft) | Depth (m) | θg (%) | ρb (g/cm3) | θv (%) | Tuff Dry wt. (g) | Cl- µg/g | Pore H2O (L) | Cl- (mg) | Cl- (mg/L) | Interval (m) | Interval Clswi (g/m2) | Cum. Clswi (g/m2) | Interval θd (m) | Cum θd (m) | Age (yrs) |
|---|---|---|---|---|---|---|---|---|---|---|---|---|---|---|---|
| 220.8 | 67.3 | 1.64 | 2.02 | 3.3 | 101.1 | 3.91 | 0.002 | 0.40 | 238 | 1.5 | 11.8 | 328 | 0.05 | 2.2 | 2831 |
| 222.7 | 67.9 | 2.16 | 2.02 | 4.4 | 101.2 | 3.56 | 0.002 | 0.36 | 165 | 0.5 | 3.6 | 332 | 0.02 | 2.2 | 2862 |
| 227.5 | 69.3 | 2.88 | 1.93 | 5.6 | 95.2 | 3.89 | 0.003 | 0.37 | 135 | 2.0 | 15.0 | 347 | 0.11 | 2.3 | 2992 |
| 234.9 | 71.6 | 2.47 | 1.69 | 4.2 | 103.1 | 4.07 | 0.003 | 0.42 | 165 | 2.0 | 13.8 | 361 | 0.08 | 2.4 | 3111 |
| 240.5 | 73.3 | 2.36 | 1.7 | 4.0 | 98.8 | 4.40 | 0.002 | 0.44 | 187 | 2.0 | 15.0 | 376 | 0.08 | 2.5 | 3240 |
| 245.5 | 74.8 | 4.28 | 1.7 | 7.3 | 101.3 | 5.29 | 0.004 | 0.54 | 124 | 1.0 | 9.0 | 385 | 0.07 | 2.6 | 3317 |
| 248 | 75.6 | 5.88 | 1.81 | 10.6 | 92.5 | 6.46 | 0.005 | 0.60 | 110 | 1.0 | 11.7 | 396 | 0.11 | 2.7 | 3418 |
| 254.1 | 77.4 | 1.94 | 1.81 | 3.5 | 98.1 | 4.63 | 0.002 | 0.45 | 239 | 1.0 | 8.4 | 405 | 0.04 | 2.7 | 3490 |
| 255.8 | 78.0 | 2.75 | 1.81 | 5.0 | 109.3 | 4.71 | 0.003 | 0.51 | 171 | 1.0 | 8.5 | 413 | 0.05 | 2.8 | 3564 |
| 259.6 | 79.1 | 1.9 | 1.89 | 3.6 | 100.5 | 4.52 | 0.002 | 0.45 | 238 | 1.0 | 8.5 | 422 | 0.04 | 2.8 | 3637 |
| 264 | 80.5 | 2.5 | 1.69 | 4.7 | 102.4 | 4.86 | 0.003 | 0.50 | 195 | 1.0 | 9.2 | 431 | 0.05 | 2.8 | 3717 |
| 269 | 82.0 | 3.18 | 1.88 | 6.0 | 106.8 | 5.43 | 0.003 | 0.58 | 171 | 1.5 | 15.3 | 446 | 0.09 | 2.9 | 3849 |
| 274 | 83.5 | 2.69 | 1.85 | 5.0 | 105.7 | 5.46 | 0.003 | 0.58 | 203 | 1.0 | 10.1 | 457 | 0.05 | 3.0 | 3936 |
| 279.4 | 85.2 | 3.44 | 1.85 | 6.4 | 99.5 | 6.53 | 0.003 | 0.65 | 190 | 1.5 | 18.1 | 475 | 0.10 | 3.1 | 4092 |
| 285 | 86.9 | 3.04 | 1.93 | 5.9 | 85.5 | 6.88 | 0.003 | 0.59 | 226 | 1.5 | 19.9 | 495 | 0.09 | 3.2 | 4264 |
| 289.5 | 88.2 | 4.54 | 1.8 | 8.2 | 96.4 | 6.81 | 0.004 | 0.66 | 150 | 1.5 | 18.4 | 513 | 0.12 | 3.3 | 4422 |
| 295.1 | 89.9 | 2.96 | 1.71 | 5.1 | 69.2 | 7.53 | 0.002 | 0.52 | 254 | 1.5 | 19.3 | 532 | 0.08 | 3.4 | 4589 |
| 301.1 | 91.8 | 2.44 | 1.73 | 4.2 | 100.8 | 7.26 | 0.002 | 0.73 | 297 | 1.5 | 18.8 | 551 | 0.06 | 3.4 | 4751 |
| 309.2 | 94.2 | 2.82 | 1.6 | 4.5 | 89.1 | 7.88 | 0.003 | 0.70 | 280 | 2.0 | 25.2 | 576 | 0.09 | 3.5 | 4969 |
| 312.5 | 95.3 | 2.88 | 1.54 | 4.4 | 102.3 | 7.55 | 0.003 | 0.77 | 262 | 3.5 | 40.7 | 617 | 0.16 | 3.7 | 5320 |
| 324.8 | 99.0 | 2.95 | 1.54 | 4.5 | 93.3 | 9.25 | 0.003 | 0.86 | 313 | 4.0 | 57.0 | 674 | 0.18 | 3.8 | 5811 |
| 344.2 | 104.9 | 7.68 | 1.4 | 10.8 | 18.3 | 12.16 | 0.001 | 0.22 | 158 | 5.0 | 85.1 | 759 | 0.54 | 4.4 | 6544 |
| 363.8 | 110.9 | 9.8 | 1.35 | 13.2 | 45.6 | 7.40 | 0.004 | 0.34 | 76 | 4.0 | 40.0 | 799 | 0.53 | 4.9 | 6889 |
| 372 | 113.4 | 9.59 | 1.4 | 13.4 | 105.8 | 4.69 | 0.010 | 0.52 | 51 | 3.0 | 20.5 | 820 | 0.40 | 5.3 | 7066 |
| 378.4 | 115.3 | 15.18 | 1.31 | 19.9 | 41.2 | 5.06 | 0.006 | 0.21 | 33 | 2.0 | 13.3 | 833 | 0.40 | 5.7 | 7180 |
| 384 | 117.0 | 12.67 | 1.3 | 16.5 | 57.3 | 3.81 | 0.007 | 0.22 | 30 | 1.5 | 7.4 | 840 | 0.25 | 6.0 | 7244 |
| 386.2 | 117.7 | 9.08 | 1.3 | 11.8 | 76.5 | 3.28 | 0.007 | 0.25 | 36 | 0.5 | 2.1 | 842 | 0.06 | 6.0 | 7263 |
| 392.5 | 119.6 | 10.45 | 1.24 | 13.0 | 46.0 | 4.15 | 0.005 | 0.19 | 40 | 2.0 | 10.3 | 853 | 0.26 | 6.3 | 7351 |
| 395 | 120.7 | 8.56 | 1.24 | 10.6 | 63.0 | 3.26 | 0.005 | 0.21 | 38 | 1.0 | 4.0 | 857 | 0.11 | 6.4 | 7386 |
| 400.6 | 122.1 | 8.54 | 1.2 | 10.2 | 58.9 | 3.48 | 0.005 | 0.21 | 41 | 1.0 | 4.2 | 861 | 0.10 | 6.5 | 7422 |
| 405.2 | 123.5 | 7.27 | 1.2 | 8.7 | 45.8 | 3.65 | 0.003 | 0.17 | 50 | 2.0 | 8.8 | 870 | 0.17 | 6.7 | 7498 |
| 419.2 | 127.8 | 8.2 | 1.2 | 9.8 | 35.4 | 3.15 | 0.003 | 0.11 | 38 | 2.0 | 7.6 | 877 | 0.20 | 6.9 | 7563 |

Appendix 1b. Borehole TDBM-1 chloride mass balance data.

| Depth (ft) | Depth (m) | θg (%) | ρb (g/cm3) | θv (%) | Tuff Dry wt. (g) | Cl- µg/g | Cl- (mg/L) | Interval (m) | Interval Clswi (g/m2) | Cum. Clswi (g/m2) | Interval θd (m) | Cum θd (m) | Age (yrs) |
|---|---|---|---|---|---|---|---|---|---|---|---|---|---|
| 2 | 0.6 | 16 | 1.3 | 20.8 | 50.56 | 5.31 | 33 | 1 | 7 | 7 | 0.21 | 0.21 | 59 |
| 4 | 1.2 | 13 | 1.3 | 16.9 | 52.25 | 31.81 | 245 | 0.5 | 21 | 28 | 0.08 | 0.3 | 238 |
| 5 | 1.5 | 6.61 | 1.3 | 8.6 | 229.2 | 20.85 | 316 | 0.4 | 11 | 38 | 0.03 | 0.3 | 331 |
| 6 | 1.8 | 12.15 | 1.3 | 15.8 | 280.1 | 48.64 | 400 | 0.3 | 19 | 57 | 0.05 | 0.4 | 495 |
| 7 | 2.1 | 4.14 | 1.3 | 5.4 | 340.0 | 15.89 | 384 | 0.3 | 6 | 64 | 0.02 | 0.4 | 548 |
| 8 | 2.4 | 4.51 | 1.3 | 5.9 | 316.9 | 15.17 | 337 | 0.5 | 10 | 73 | 0.03 | 0.4 | 633 |
| 10 | 3.0 | 1.58 | 1.3 | 2.0 | 255.9 | 4.58 | 291 | 0.4 | 2 | 76 | 0.01 | 0.4 | 654 |
| 11 | 3.4 | 1.48 | 1.3 | 1.9 | 323.1 | 3.80 | 256 | 0.3 | 1 | 77 | 0.01 | 0.4 | 666 |
| 12 | 3.7 | 1.64 | 1.3 | 2.1 | 313.4 | 4.08 | 249 | 1.0 | 5 | 83 | 0.02 | 0.5 | 712 |
| 15 | 4.6 | 1.12 | 1.3 | 1.5 | 286.8 | 1.69 | 151 | 1.0 | 2.2 | 85 | 0.01 | 0.5 | 731 |
| 17 | 5.2 | 1 | 1.3 | 1.3 | 46.2 | 1.351 | 135 | 1.0 | 1.8 | 87 | 0.01 | 0.5 | 746 |
| 25 | 7.6 | 1 | 1.3 | 1.3 | 50.0 | 4.35 | 435 | 1.0 | 5.7 | 92 | 0.01 | 0.5 | 795 |
| 28 | 8.5 | 1 | 1.3 | 1.3 | 298.9 | 4.25 | 423 | 1.0 | 5.5 | 98 | 0.01 | 0.5 | 843 |
| 31 | 9.4 | 1.57 | 1.3 | 2.0 | 263.9 | 0.77 | 49 | 1.0 | 1.0 | 99 | 0.02 | 0.5 | 851 |
| 33 | 10.1 | 1.95 | 1.3 | 2.5 | 252.3 | 2.19 | 112 | 1.5 | 4.3 | 103 | 0.04 | 0.6 | 888 |
| 44 | 13.4 | 2 | 1.3 | 2.6 | 50.7 | 5.51 | 276 | 2.5 | 17.9 | 121 | 0.07 | 0.6 | 1042 |
| 49 | 14.9 | 1.57 | 1.3 | 2.0 | 439.2 | 9.87 | 616 | 2.5 | 31.4 | 152 | 0.05 | 0.7 | 1313 |
| 54 | 16.5 | 2 | 1.3 | 2.6 | 47.6 | 10.53 | 528 | 2.0 | 27.4 | 180 | 0.05 | 0.7 | 1549 |
| 59 | 18.0 | 1.86 | 1.3 | 2.4 | 411 | 9.38 | 505 | 2.0 | 24.4 | 204 | 0.05 | 0.8 | 1760 |
| 64 | 19.5 | 2 | 1.3 | 2.6 | 54.9 | 18.1 | 905 | 2.0 | 47.1 | 251 | 0.05 | 0.8 | 2165 |
| 74 | 22.6 | 1.51 | 1.4 | 2.1 | 308.3 | 15.5 | 1028 | 2.0 | 43.4 | 295 | 0.04 | 0.9 | 2539 |
| 79 | 24.1 | 2.42 | 1.65 | 4.0 | 349.4 | 25.96 | 1074 | 1.5 | 64.2 | 359 | 0.06 | 0.9 | 3093 |
| 84 | 25.6 | 2.0 | 1.65 | 3.3 | 53.1 | 31.39 | 1570 | 2.5 | 129.5 | 488 | 0.08 | 1.0 | 4209 |
| 99 | 30.18 | 1.76 | 1.65 | 2.9 | 428.0 | 17.57 | 999 | 3.0 | 87.0 | 575 | 0.09 | 1.1 | 4959 |
| 109 | 33.2 | 1 | 1.65 | 1.7 | 51.5 | 9.39 | 939 | 2.0 | 31.0 | 606 | 0.03 | 1.1 | 5227 |